Articles

Kinases, Homology Models, and High Throughput Docking

David J. Diller* and Rixin Li

Pharmacopeia, Inc., CN5350, Princeton, New Jersey 08543-5350

Received November 5, 2002

With the many protein sequences coming from the genome sequencing projects, it is unlikely that we will ever have an atomic resolution structure of every relevant protein. With high throughput crystallography, however, we will soon have representative structures for the vast majority of protein families. Thus the drug discovery and design process will rely heavily on protein modeling to address issues such as designing combinatorial libraries for an entire class of targets and engineering genome-wide selectivity over a target class. In this study we assess the value of high throughput docking into homology models. To do this we dock a database of random compounds seeded with known inhibitors into homology models of six different kinases. In five of the six cases the known inhibitors were found to be enriched by factors of 4−5 in the top 5% of the overall scored and ranked compounds. Furthermore, in the same five cases the known inhibitors were found to be enriched by factors of 2−3 in the top 5% of the scored and ranked known kinase inhibitors, thus showing that the homology models can pick up some of the crucial selectivity information.

Introduction

Homology modeling has the potential to impact the drug development cycle significantly in at least the following three ways. First, whether due to limited resources or problems with protein crystallization, X-ray structures often become available too late in the drug design process to have maximal impact. This limits the impact that structure-based drug design has on drug development. As homology models are relatively inexpensive to create, they could fill the gap between the start of drug discovery and the elucidation of the target structure by experimental methods. Second, in designing combinatorial libraries for high throughput screening, often one is interested in entire target families, for example kinases, G-protein-coupled receptors, nuclear hormone receptors, etc., rather than a single target. In target families where a single genome could have hundreds of members, it is unlikely that we will ever have structures of every family member. Homology models could fill in the resulting gaps, thereby allowing true class-based design of combinatorial libraries using structure-based methods. Third, it seems likely that many toxicity failures have been due to lack of selectivity. An example is the gastrointestinal agent Cisapride which was withdrawn from the market because of cardiotoxicity.[1] The cardiotoxicity of Cisapride was subsequently determined to be caused by potent inhibition of the human ether-a-go-go-related gene potassium channel.[2] With the sequencing of the human genome now complete, homology modeling might offer an avenue through which genome wide selectivity, particularly over target classes, could be addressed.

Since homology modeling has the potential to impact the design of drugs in so many ways, it is important to assess the quality of the information one can obtain from homology models and to understand how best to extract this information. Given the wide range of potential problems addressable with homology modeling, it is important to understand which problems are amenable to homology modeling.

For this study the tyrosine and serine/threonine kinase family was chosen. Protein kinases represent a good test family for homology modeling for a variety of reasons. First, kinases are becoming a very important class of drug targets. They have been implicated in many diseases including cancer[3], angiogenesis[3], Alzheimer's disease,[4−6] diabetes,[7,8] and inflammation.[9,10] With the approval of the first kinase-targeted drugs,[11] the interest in kinases and thus our understanding of their role in disease will continue to grow.

Second, the human genome contains a large number of protein kinases. Recently, using a hidden Markov model, Manning and colleagues[12] have located 518 distinct human kinase genes from all available sources including public and Celera genomic databases. As a result, selectivity is crucial for any potential kinase-targeted drug. Thus, the design of kinase-targeted drugs could benefit significantly from large scale homology modeling.

Third, there are many publicly available X-ray structures of a variety of kinases. In the protein data bank[13] there are over 150 X-ray structures of kinase catalytic domains. The kinases that currently have publicly available structures include the tyrosine kinases ABL (1fpu), BTK (1k2p), CSK (1byg), EGFR (1m14), EPHB2 (1jpa), FGFr1 (1agw), FGFr2 (1gjo), HCK (1ad5), IGF1r (1k3a), INSr (1gag), LCK (1qpc), MUSK (1luf), SRC

* To whom correspondence should be addressed: ddiller@pharmacop.com (e-mail), (609) 452-3783 (phone), (732) 422-0156 (fax).

10.1021/jm020503a CCC: $25.00 © 2003 American Chemical Society
Published on Web 09/20/2003

Figure 1. The basic kinase structure. The N-terminal domain is shown is green. The C-terminal domain is shown in purple. The hinge region is shown in light blue. ATP is shown in red. The substrate peptide is shown in yellow. The structure used is pdb code 1ir3.[76]

(1fmk), TIE2 (1fvr), and VEGFr2 (1vr2) and the ser/thr kinases AKT2 (1o6k), CAMK1 (1a06), CDK2 (1aq1), CDK5 (1h4l), CDK6 (1bl7), CHK1 (1ia8), CSNK1D (1cki), CSNK2A1 (1jwh), DAPK (1ig1), ERK2 (1erk), GSK3β (1gng), JNK3 (1jnk), MAPKAPK2 (1kwp), P38α (1a9u), P38γ (1cm8), PAK1 (1f3m), PHKG1 (1phk), PKA (1apm), and TGFβ1r (1b6c). Beyond the relative abundance of kinase structures, they also have a common template. The kinase fold consists of two domains, an N-terminal domain and a C-terminal domain connected by a stretch of 5−6 residues called the hinge region[14] (see Figure 1). The ATP binding site is the cleft formed between the two domains.

From a computational viewpoint, kinases represent a very difficult and thus interesting challenge. In general, the structures have a wide range of flexibility. This flexibility includes a wide range of side chain motion in the ATP binding site, flexible loops such as the active site loop and the activation loop, and domain motion between the N and C terminal domains. This binding site variation depends on the actual kinase, the nature of the cocrystallized ligand, the activation state, and crystal contacts. Typically, the interkinase structural variation is not significantly more than the intrakinase structural variation.

In this study we specifically looked at whether high throughput docking can be used with homology models. To assess the potential of homology models in the docking arena, homology models were built for six different kinases using a variety of templates. Data sets of known inhibitors of the six kinases were assembled from the literature. A database of 32 000 random compounds was then assembled. The random compounds and the inhibitors were docked into the homology models using LibDock.[15] The results were then analyzed to see if the known inhibitors could be pulled out over the random compounds. In 5/6 cases the

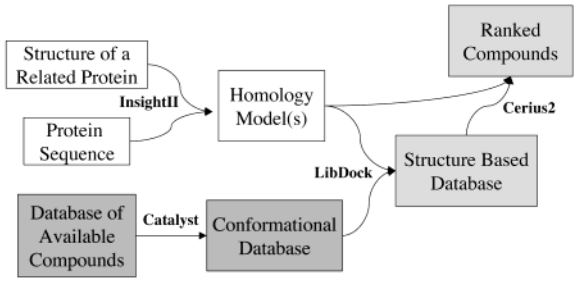

Figure 2. A flowchart of the homology modeling/docking process. First, a homology model is built for the desired protein using a related template and the program Modeler[16,17] available through Insight2000.[18] The compounds of interest were converted to a conformational database using Catalyst.[19] The conformations were then docked into the homology model using LibDock.[15] The docked compounds were then ranked using the scoring suite available in Cerius2.[21]

inhibitors could be pulled out at a rates around a factor of 5 faster than the random compounds. In the sixth case, the inhibitors were pulled out no faster than the random compounds. When rerun with a homology model built from an alternate template, the results in this sixth case were comparable to the first five cases. In addition, in all cases the homology models were able to pull out the appropriate kinase inhibitors around 2 times faster when compared to the other kinase inhibitors. Thus, the models are picking up some of the selectivity information.

Methods

The basic process (see Figure 2) followed throughout this study is that homology models were built using Modeler[5,16,17] accessible through the Insight2000[18] interface. Conformational databases were built for the compounds of interest using Catalyst.[19] The compounds were then docked into the homology models using LibDock.[15] The docked compounds were then ranked using the piecewise linear potential2[20] as implemented in Cerius2[21] augmented with a solvation and entropy correction.

As described in the preceding section, protein kinases were chosen as a test family. The six kinases chosen were the epidermal growth factor receptor (EGFr), the fibroblast growth factor receptor (FGFr1), the vascular endothelial growth factor receptor (VEGFr1), the platelet-derived growth factor receptor (PDGFrβ), the mitogen-activated protein kinase P38, and the non receptor tyrosine kinase SRC. The particular kinases were selected largely because a sufficiently large number of inhibitors could be assembled for each from the literature. The templates used to build the homology models offer a wide range of sequence identities (see Table 1). In addition, some of the models were built from a single template while others were built using multiple templates. The models were built using the default options from the Insight2000 interface.

A database of over 1000 kinase inhibitors was assembled from the literature (see Table 2). The kinase inhibitor sets include inhibitors of EGFr, VEGFr1, PDGFrβ, FGFr1, SRC, and P38[22−63] (see Figure 3 for representative structures). The data set of kinase inhibitors is not ideal. In particular, the selectivity information for each inhibitor is not known across all six kinases. As a first example, the SmithKline series

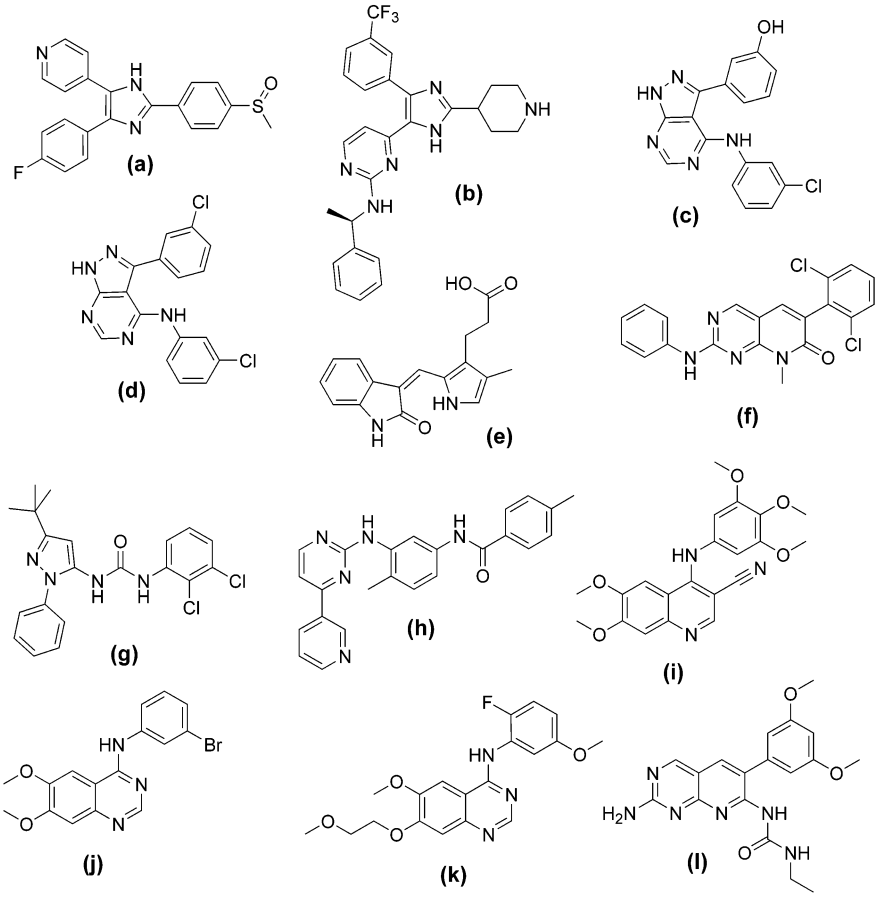

Figure 3. Representative kinase inhibitors used in the docking study. The kinase data set consisted of 141 compounds in the same class as **3a** and **3b**, 69 in the same class as **3c**, 42 in the same class as **3e**, 110 in the same class as **3f**, 5 in the same class as **3g**, 38 in the same class as **3h**, 302 in the same class as **3I**, **3j**, and **3k**, and 173 in the same class as **3l**. A few miscellaneous classes of compounds, such as purines, were members of the data set as well.

Table 1. Kinases in the Docking Study and the Templates Used To Build the Homology Models[a]

kinase	templates	seq. i.d., %	X-ray
	FGFr1 (1agw)	53	
PDGFrβ	VEGFr2 (1vr2)	55	none
	INSr (1ir3)	35	
VEGFr1	VEGFr2 (1vr2)	77	none
	FGFr1 (1agw)	55	
	FGFr1 (1agw)	34	
	CSK (1bgy)	35	
EGFr	INSr (1ir3)	30	1m14
	VEGFr2 (1vr2)	33	
	HCK (1qcf)	33	
	LCK (3lck)	31	
P38	ERK (3erk)	49	1a9u
SRC	LCK (3lck)	66	2src
	ABL (1fpu)	48	
	VEGFr2 (1vr2)	58	
FGFr1	INSr (1ir3)	38	1agw
	SRC (2src)	38	

[a] Structures were eliminated as potential templates if they were not complete in the ATP binding site or the ATP binding site was hindered by a loop such as the activation loop. The sequence identities reported are over the entire kinase domain.

Table 2. Molecules Used in the Study and Their Physical Properties

	no.[a]	MW[a]	rotatable bonds[a]	H-bond acceptor[a]	H-bond donor[a]
PDGFrβ	161	368 ± 97	5.3 ± 2.6	4.6 ± 1.6	1.2 ± 1.2
EGFr	387	355 ± 64	4.2 ± 2.4	4.6 ± 1.4	2.0 ± 1.1
VEGFr1	46	383 ± 49	6.2 ± 1.9	5.6 ± 1.9	1.9 ± 1.1
P38	115	366 ± 44	4.7 ± 1.5	4.5 ± 1.1	1.3 ± 1.1
SRC	138	426 ± 76	6.1 ± 2.6	5.9 ± 1.2	2.2 ± 1.3
FGFr1	111	438 ± 72	6.5 ± 2.7	5.8 ± 1.3	2.2 ± 1.2
random		357 ± 38	9.1 ± 2.9	4.6 ± 1.2	2.0 ± 1.2

[a] The value given is the mean ± the standard deviation.

of P38 inhibitors has shown some inhibition of LCK[35] (Figure 3a), a member of the SRC family. Other members of this series, however, have been shown to be quite selective versus LCK[38] (Figure 3b) and thus will likely be selective versus SRC. Most of the members of this class of P38 inhibitors do not have published binding data versus SRC or any of the other members of the test family. It is reasonable to believe that the P38 inhibitors are more potent versus P38 on average than the remaining kinase inhibitors. As a second example, the compound shown in Figure 3c inhibits both c-SRC and EGFr with IC_{50}s in the low nanomolar range.[60] The closely related compound shown in Figure 3d is over 100 fold selective for EGFr versus c-SRC.[60] Thus, while there is certainly some cross inhibition between the inhibitors of the data set, there should be a sufficient amount of differentiation between the various kinase inhibitor sets to draw some conclusions concerning the potential for homology models to address kinase selectivity.

These kinase inhibitors were then used as seeds in a database of 32 000 random compounds. The random compounds were selected from our internal collection with some attempt to keep the polarity and molecular weight in line with the kinase inhibitors. The reason for doing this is to ensure that the homology models do not select the kinase inhibitors solely based on size. The

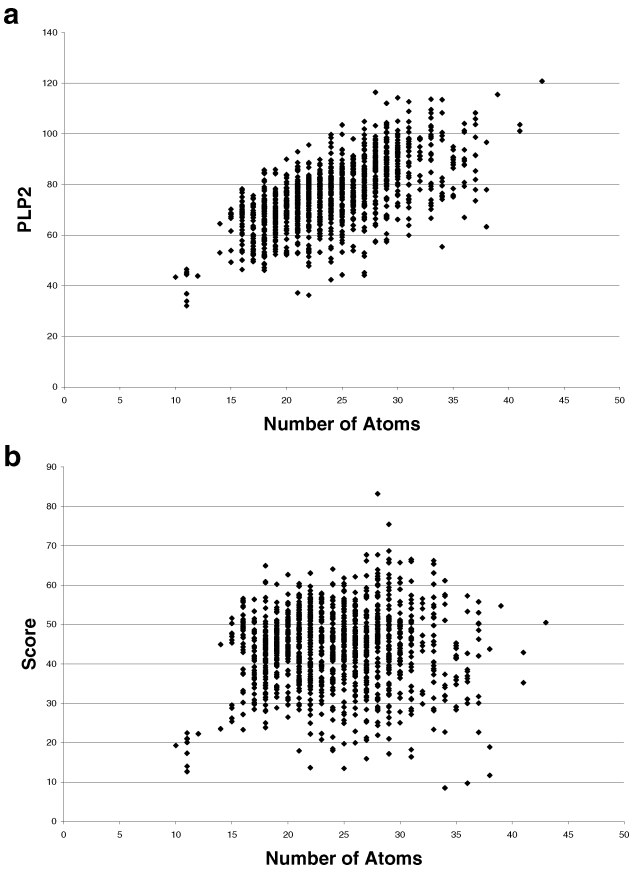

Figure 4. A plot of the size of the molecule versus its docked score. **4a**: With the PLP alone a large correlation between size and score is observed (typically R^2 of about 0.6). **4b**: The PLP score adjusted with solvation and entropy corrections.

physical properties of the inhibitors and the random compounds are shown in Table 2. The entire database of compounds was turned into a conformational database using the program Catalyst[19] with a maximum of 100 conformations per compound and a 15 kcal/mol strain cutoff.

The compounds were then docked using LibDock with a standard set of parameters.[15] Docking times range from 2 to 5 s per compound. The box size for each kinase was 22 Å × 22 Å × 15 Å with the *X*-axis running parallel to the hinge, the *Y*-axis running parallel to the active site loop and the *Z*-axis (the short axis) running from the C-terminal domain to the N-terminal domain. Each compound was docked multiple ways in the binding site, but only the top ranked pose by LibDock's internal score was used in the final scoring stage.

The compounds were ranked using the Piecewise Linear Potential 2 (PLP2)[20] augmented with a solvation and entropy correction. The PLP2 score was chosen because it has in the past given us the most consistent results. The shortcoming of the PLP2 score and many widely used scoring functions is that it primarily counts interactions. The result is that the score is often correlated heavily with the size of the compounds (see Figure 4a). The correlation between score and size makes it difficult to extract any meaningful information from the docking scores. To offset this correlation, the score has for this study been augmented with a solvation and entropy correction. The entropy correction was set at 0.5 kcal/mol per rotatable bond, as this seems to be a well supported value.[64−67] The solvation model used

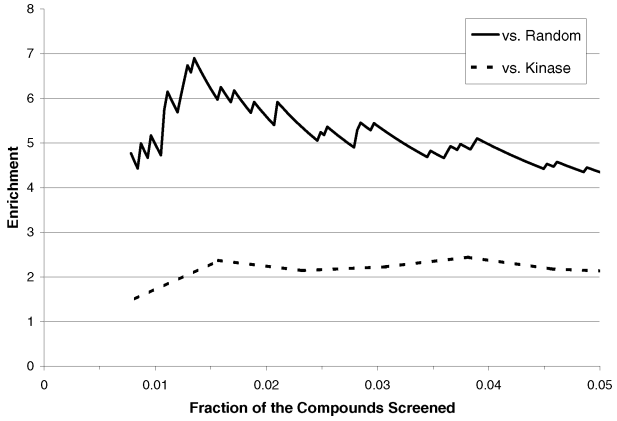

Figure 5. The results with the PDGFrβ homology model. The solid curve shows the enrichment of the PDGFrβ inhibitors versus the random compounds. The dashed curve shows the enrichment of the PDGFrβ inhibitors versus the other kinase inhibitors.

is that described by Stouten and co-workers.[68] The chief advantage of this solvation model is that it uses only an atom pairwise potential, which means the protein contribution to the solvation can be precalculated on grids making the score extremely fast to calculate. The solvation model was weighted to remove the correlation between the resulting score and molecular weight (see Figure 4b).

The scores were then used to see if the known inhibitors for each kinase could be pulled out from the random compounds and from the other known kinase inhibitors. The quantity used to measure the quality of the docking results is the enrichment.[69] The enrichment is defined via

$$\text{enrichment} = \frac{a/n}{A/N} \qquad (1)$$

where N is the number of compounds, n is some predetermined number of compounds to be screened, A is the number of actives in the entire collection, and a is the number of actives in the top n ranked compounds. Enrichments greater than one indicate a successful docking experiment. Generally we will give the range of enrichments over 1−5% of the total compounds.

Results

As a typical example the results with the PDGFrβ homology model are shown in Figure 5. The maximum enrichment found is 6.9. This enrichment occurs when about 1.5% of the compounds have been screened. Between 1% and 5% of the compounds screened the enrichment versus the random compounds varies between 4.5 and 6.9. To test whether the homology models can pick up more than just the general kinase shape, the enrichment of the PDGFrβ inhibitors was considered against the other kinase inhibitors. Against the kinase compounds the PDGFrβ enrichment is approximately 2 over the 1% to 5% of the kinase compounds screened. This latter result is of significance because it means the homology model is picking up some of the specific information, and thus the docking results contain some information concerning selectivity.

The overall results for the six kinases are shown in Table 3. The table gives the maximum and minimum

Table 3. Overall Results[a]

	homology model		X-ray structures	
kinase	random	kinase	random	kinase
PDGFrβ	4.8−6.9	1.6−2.4	NA	NA
VEGFr1	4.2−7.5	1.4−2.1	NA	NA
EGFr	3.9−5.1	1.3−1.6	4.8−6	1.5−1.8
P38	1.5−2.6	2.0−2.8	6.9−11.5	1.5−5.3
SRC	10.8−38.6	3.0−8.0	3.2−5.3	1.8−2.5
FGFr1	1.0−1.0	1.0−1.0	1.0−1.0	1.0−1.0

[a] The EGFr study with the X-ray structure was redone with a comparable set of random compounds drawn from the MDDR database. The observed enrichments ranged from 3.0 to 3.5.

enrichments versus the random compounds and versus the other kinase inhibitors in the top ranked 1−5% of the compounds. For the second homology model where no crystal structure is available (VEGFr1), the results are comparable to the PDGFrβ case. The enrichment versus random compounds ranges from a lower limit of around 4 to an upper limit of around 7. For the VEGFr1 case the enrichment versus the kinase compounds varies from 1.4 to 2.1.

For the four cases where an X-ray structure was available (EGFR, P38, SCR, FGFr1), the same docking experiment was performed for the homology model and for the X-ray structure to determine how much loss of information was due to the homology models. For these four cases the results, described below, are instructive.

For EGFr, an apo-structure (1m14[70]) was used. In this case, the results with the homology model and the X-ray structure are comparable. The homology model exhibited enrichments between 4 and 5 versus the random compounds compared to enrichments between 5 and 6 for the X-ray structure. When compared to the other kinase inhibitors, the enrichments are 1.3−1.6 for the homology model and 1.5−1.8 for the X-ray structure. While the enrichments versus the kinase compounds seem low, nearly one-third are known EGFr inhibitors. Thus the maximum enrichment is only 3.

For the P38 case, the docking experiments gave the results that one from the outset would have expected. The X-ray structure worked quite well. The enrichments ranged from 7 to 11.5 against the random compounds and went as high as 5 relative to the other kinase inhibitors. The homology model performed significantly worse. The enrichments varied from 1.5 to 2.6 versus the random compounds. The homology model, however, did slightly better versus the kinase compounds: enrichments in this case varied from 2.0 to 2.8. Part of the reason for the superior performance of the X-ray structure is that the structure used (pdb code 1a9u[71]) was solved in complex with the Smith Kline inhibitor SB203580 (Figure 3a). Since the majority of the P38 inhibitors are from the same class there is likely some bias toward this series.

For SRC, the homology model worked surprisingly well. The enrichment versus the random compounds ranged from 10 up to nearly 40. In fact the three highest scoring compounds for this case are all SRC inhibitors. The SRC X-ray structure was not nearly as productive: the enrichment versus the random compounds varied from 3 to 5. While the enrichment for the X-ray structure is in line with the majority of the homology models, it is quite a bit less than that of the SRC homology model. The reason for the relatively poor

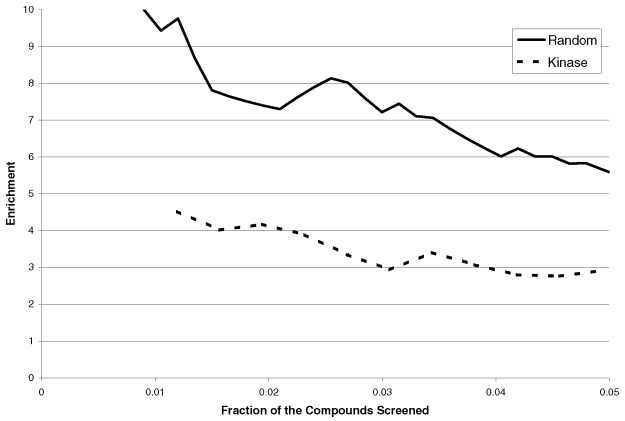

Figure 6. The results with the FGFr1 homology model built from an alternate template. The curves are as those defined in Figure 5.

performance of the SRC X-ray structure is in part due to the fact that this particular structure was solved in complex with ANP. The kinase structures solved in complex with ATP analogues in general tend to be more closed than other structures and as a result typically do not work as well for this purpose. The reason the SRC homology model worked so well is not clear. In part, the template (pdb structure 3lck[72]) used to build the model is an LCK structure, which is a member of the SRC family. The overall identity of the two proteins is 66%. In all likelihood the template would work as well as the homology model. The LCK structure used as a template, however, is an apo structure. Thus, there is no issue of bias to any series of compounds.

For FGFr1, neither the homology model nor the X-ray structure was able to extract the FGFr1 inhibitors above random. The X-ray structure was solved in complex with a relatively small inhibitor (Figure 3c). This inhibitor appears to have led to a significant amount of induced fit, resulting in a binding site that was much to small to accommodate the majority of the FGFr1 inhibitors. A second homology model was created using an alternate template (pdb3lck which is 39% identical to FGFr1). In this case the docking experiment was more consistent with the VEGFr1, EGFr, and PDGFrβ cases. With this new homology model the enrichment versus random varied between 5.5 and 10, and the enrichment versus the kinase compounds ranged between 2.8 and 4.5 (see Figure 6). It is not absolutely clear why this second homology model worked well while the original model failed. The major difference appears to be that the second model is more open than the first model.

The overall results with the four X-ray structures can be explained. The P38 X-ray structure, which worked significantly better than the majority of the homology models, was cocrystallized with a ligand that was representative of the majority of the ligands in the p38 inhibitor set. The SRC structure, which performed comparable to the majority of the homology models, was cocrystallized with an ATP analogue. Similarly, the EGFr structure, which is an apo structure, performed comparably to the homology models. The FGFr1 X-ray structure, which resulted in no enrichment, was cocrystallized with a ligand that was not representative of the majority of the ligands in the FGFr1 data set. Thus, the nature of the bound ligand can significantly bias the results of docking. Not surprisingly, when the bound

ligand is similar to the inhibitors of interest, the cocrystal structure will in all likelihood prove superior. When the bound ligand is significantly different from the inhibitors of interest, the cocrystal structure might not be the most appropriate. Thus, when one is interested in discovering novel chemotypes, apo structures should be considered as viable alternatives to structures with bound ligands.

A systematic comparison of the predicted binding modes of the docked compounds is very difficult because the binding modes for most of the series are not known. A visual inspection of the results did reveal a clear trend. The cases with the best enrichment corresponded to those in which the compounds were docked the most consistently. As an example, the series of SRC inhibitors with representative shown in Figure 3f was consistently docked with the 2,6-dichlorophenyl in the main hydrophobic pocket, a nitrogen of the central bicyclic system hydrogen bonding to the NH of Met343 of the hinge region, and the remaining phenyl in the secondary hydrophobic patch. While the true binding mode of this series of inhibitors is not known for SRC, it is consistent with the known structure−activity relationship.[24,37,57] As the enrichment decreased, typically the binding modes were both less consistent and less convincing. For example, one compound might be docked with an appropriate group in the hydrophobic pocket but not interact with the NH of the hinge region while a second compound would be docked with the interaction with the NH of the hinge region but miss the main hydrophobic pocket. Finally, compounds such as those shown in Figure 3g and 3h are known to cause large degrees of induced fit on the part of the protein and could never be accurately docked into the given homology models.[73,74]

The majority of the P38 inhibitors used in this study are in the same class as those shown in Figure 3a,b. Of the 115 P38 inhibitors used in this study 63 have the triaryl pyridine-imidazole-phenyl core. The binding mode for this series of compounds is well understood (see pdb structures 1a9u, 1bl6, and 1bl7[71]). Thus the quality of the P38 docking studies can be further quantified by comparing the docked poses of the core of each of the compounds with the triaryl core to the crystallographically determined binding mode for this core in P38. For both the study with the X-ray structure and the study with the homology model, the majority (∼80%) of the compounds have a pose which exhibits an rms deviation below 2.0 Å (see Figure 7a). The difference between the two cases is that in the study with the X-ray structure the majority of the compounds attain an rms deviation below 1.0 Å, whereas for the homology model, the rms deviations vary between 1.0 Å and 2.0 Å. The difference in the docking quality in all likelihood accounts for the difference in the observed enrichments.

The rms deviation alone can be somewhat misleading. As mentioned above, both P38 structures 1a9u and 1bl6 are cocrystallized with inhibitors containing the triaryl core. When aligned, the C_α rms deviation in the ATP binding site is very small (∼0.3 Å). The rms deviation of the triaryl cores from the resulting alignment is 1.1 Å (see Figure 7b). A visual examination, however, shows essentially the same interaction pattern for the core:

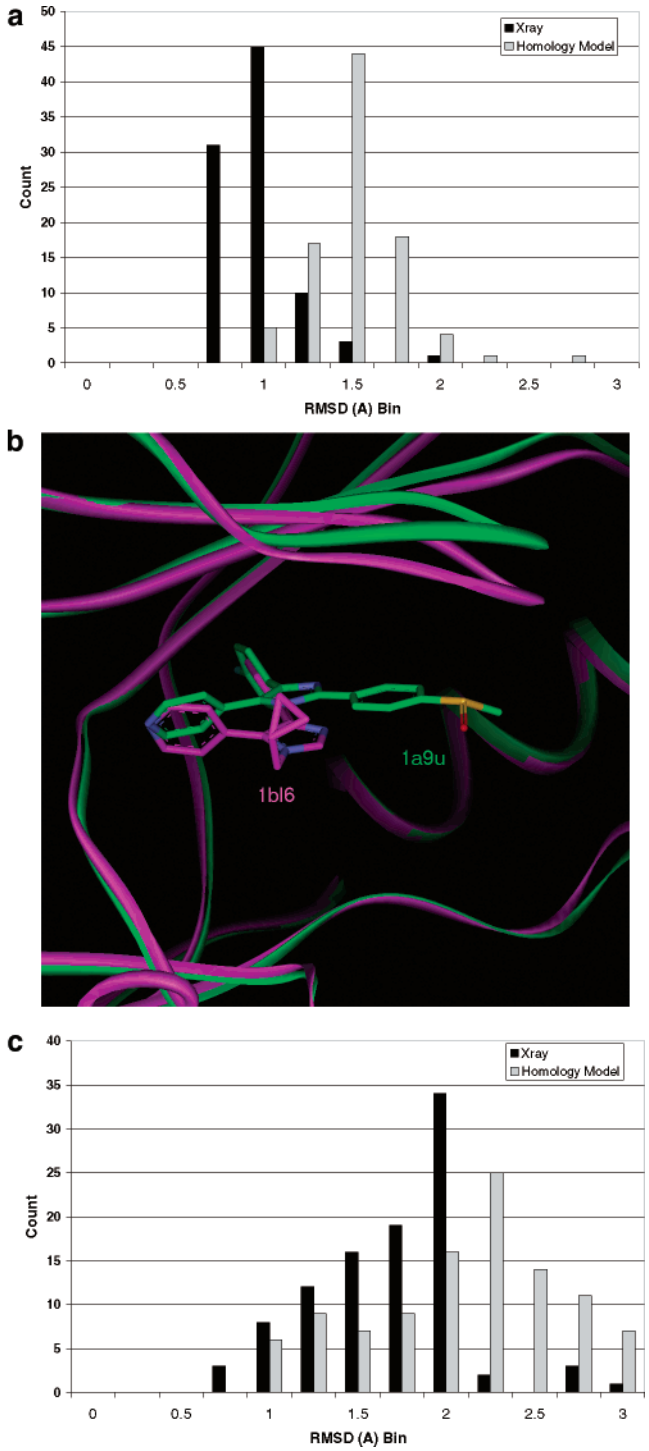

Figure 7. A comparison of the docked poses with their crystallographically determined position. **7a**: The rms deviation between the docked poses and the crystallographically determined position of the triaryl pyridine-imidazole-phenyl core of the compound shown in Figure 3a. The rms deviation was calculated only over the atoms of the triaryl core of those P38 compounds with the triaryl core. **7b**: An alignment of the two P38 X-ray structures 1a9u (green) and 1bl6 (purple). While the proteins align very well (rms deviation < 0.3 Å), the triaryl cores of the two cocrystallized ligands differ significantly (rms deviation 1.1 Å). **7c**: The rms deviation between the core of the EGFr compounds and the crystallographically determined position for the core. The core in this case is that of the molecules shown in Figure 3j,k.

the pyridine nitrogen hydrogen bonds with the NH of Met109, the central imidazole hydrogen bonds with

Lys53, and the phenyl ring binds in the main hydrophobic pocket. Even though the rms deviation is significant, the binding modes are identical. Thus the rms deviation alone is not a sufficient indication of the quality of docking.

In the P38 study, a visual inspection verifies that the reason for the difference in enrichments can be attributed to the quality of the poses. For the X-ray structure, the vast majority of the top-ranked poses make the three key interactions: the pyridine-Met109 hydrogen bond, the imidazole-Lys53 hydrogen bond, and the phenyl binding in the main hydrophobic pocket. For the homology model, usually at least one of the three interactions is significantly distorted. The difference in the quality of these interactions ultimately accounts for the difference in the observed enrichment.

In the case with EGFR, the pdb structure 1m17[70] is cocrystallized with a ligand that is representative of a large subset of the EGFR inhibitors used in this study. Of the 387 EGFR inhibitors used in this study, 111 have the same core as the molecule shown in Figures 3j and 3k. In this case the majority of the compounds have a pose that is docked reasonably well (Figure 7b). The compounds appear to be somewhat better docked than the homology model. Again, this agrees well with the fact that the X-ray structure showed slightly better enrichment than the homology model.

In the case with FGFr, the pdb structure 2fgi[75] is cocrystallized with a ligand that is representative of a large subset of the FGFr inhibitors. Of the 111 FGFr inhibitors used in this study, 61 have the same biaryl core as either the molecule shown in Figure 3f or that shown in Figure 3l. As in the P38 and EGFr cases, the quality of docking can be quantified by comparing the core of each pose of these 61 molecules to the crystallographically observed binding mode for the core. For both the original homology model and the X-ray structure used in the study, very few (<5) of the 61 molecules were docked so that the core was within a reasonable distance of the crystallographically determined position of the core. For the second homology model, 20 of the compounds had poses within 1.0 Å of the crystallographically observed binding mode for the core, and most of the compound had poses below 2.0 Å. Thus again, the observed enrichments correlate well with the observed enrichments.

Conclusions

In this study, homology models of six kinases were built to see if when combined with high throughput docking they could distinguish between known inhibitors and random compounds. In five of the six cases the models were able to select the inhibitors fives times over random. In the sixth case the original model was unable to distinguish between inhibitors and random compounds. In this case a model built with an alternate template was able to distinguish inhibitors from random at a rate comparable to the original five models. Thus, it seems reasonable with the current protocols that in the majority of cases a factor of 5 times above random is reasonable. With some enhancements, factors around 10 are within reach.

Homology models can be improved by a few general considerations. The most important consideration in building a quality homology model is to get to know the protein family of interest. The first step should always be to gather as many sequences from the family and perform a multiple sequence alignment. A bad alignment will always result in a poor homology model. A multiple sequence alignment will give the modeler some statistical confidence in the alignment and also point out potential areas of low reliability in the homology model. The second step is to align as many X-ray structures from the family as are available. The multiple structural alignment should be used first to validate the multiple sequence alignment. In particular the multiple structural alignment can improve the low confidence regions of the multiple sequence alignment. In addition, the multiple structural alignment can be used to better understand the structural degrees of freedom of the protein family. This will give the modeler a better feeling for the regions of the homology model likely to be of high error. In cases where there are not sufficient available structures to do a multiple structural alignment, site-directed mutagensis data could be used to validate the multiple sequence alignment. Another aspect to consider carefully in the homology model building process is the selection of the template. Aspects such as overall sequence identity, sequence identity in the binding site, size and location of insertions and deletions, quality of the potential templates, and inhibitors or substrates bound in the active site should all be considered. The relative weights for each of these factors are likely to be dependent on the protein family of interest. For kinases, structures with an ATP analogue are less desirable than apo structures. Structures with bound inhibitors are certainly better than an apo structure when one is interested in inhibitors of related structure to that in the cocrystal complex. When an unbiased model is desired, apo structures should be considered as well. Generally, for kinases, open structures make better templates.

At the level of quality demonstrated in this study, there are several clear places of application for homology modeling. The first is to augment X-ray crystal structures early in the drug discovery process. While homology modeling and docking will never be able to compete with the accuracy of cocrystal structures, there usually is some time lag between the discovery of inhibitors and the solution of the cocrystal complex. Thus when suitable templates are available, homology modeling should be considered a viable avenue to improve early optimization efforts. The second area of clear application of homology models is to improve target class-focused discovery libraries. Given the expense of creating large numbers of compounds, improving target class libraries by only a factor of 2 is well worth the CPU time required to do so.

The frontier for protein modeling is to address genome-wide selectivity for compounds over a target family. With our current understanding of the physics of protein folding and protein−ligand binding, addressing genome-wide selectivity is not yet within reach. Given its relative importance for kinase-targeted inhibitors and its clear scientific appeal, this problem will certainly be vigorously pursued soon.

References

(1) Vitola, J.; Vukanovic, J.; Roden, D. M. Cisapride-induced torsades de pointes. *J. Cardiovasc. Electrophysiol.* **1998**, *9*, 1109−1113.

(2) Rampe, D.; Roy, M. L.; Dennis, A.; Brown, A. M. A mechanism for the proarrhythmic effects of cisapride (Propulsid): high affinity blockade of the human cardiac potassium channel HERG. *FEBS Lett.* **1997**, *417*, 28−32.

(3) Blume-Jensen, P.; Hunter, T. Oncogenic kinase signaling. *Nature* **2001**, *411*, 355−365.

(4) Kirschenbaum, F.; Hsu, S. C.; Cordell, B.; McCarthy, J. V. Glycogen synthase kinase-3beta regulates presenilin 1 C-terminal fragment levels. *J. Biol. Chem.* **2001**, *276*, 30701−30707.

(5) Sanchez, R.; Sali, A. Comparative protein structure modeling. Introduction and practical examples with modeller. *Methods Mol. Biol.* **2000**, *143*, 97−129.

(6) Zheng, W. H.; Kar, S.; Dor, S.; Quirion, R. Insulin-like growth factor-1 (IGF-1): a neuroprotective trophic factor acting via the Akt kinase pathway. *J. Neural Transm. Suppl.* **2000**, 261−272.

(7) Winder, W. W. AMP-activated protein kinase: possible target for treatment of type 2 diabetes. *Diabetes Technol. Ther.* **2000**, 441−448.

(8) Wagman, A. S.; Nuss, J. M. Current therapies and emerging targets for the treatment of diabetes. *Curr. Pharm. Des.* **2001**, *7*, 417−450.

(9) Lee, J. C.; Kumar, S.; Griswold, D. E.; Underwood, D. C.; Votta, B. J.; Adams, J. L. Inhibition of p38 MAP kinase as a therapeutic strategy. *Immunopharmacology* **2000**, *47*, 185−201.

(10) Goepfert, T. M.; Brinkley, B. R. The centrosome-associated Aurora/Ipl-like kinase family. *Curr. Top Dev. Biol.* **2000**, *49*, 331−342.

(11) Druker, B. J.; Sawyers, C. L.; Capdeville, R.; Ford, J. M.; Baccarani, M.; Goldman, J. M. Chronic myelogenous leukemia. *Hematology* **2001**, 87−112.

(12) Manning, G.; Whyte, D. B.; Martinez, R.; Hunter, T.; Sudarsanam, S. The protein kinase complement of the human genome. *Science* **2002**, *298*, 1912−1934.

(13) Berman, H. M.; Westbrook, J.; Feng, Z.; Gilliland, G.; Bhat, T. N.; Weissig, H.; Shindyalov, I. N.; Bourne, P. E. The Protein Data Bank. *Nucleic Acids Res.* **2000**, *28*, 235−242.

(14) Toledo, L. M.; Lydon, N. B.; Elbaum, D. The structure-based design of ATP-site directed protein kinase inhibitors. *Curr. Med. Chem.* **1999**, *6*, 775−805.

(15) Diller, D. J.; Merz, K. M. High Throughput Docking for Library Design and Library Prioritization. *Proteins: Struct. Funct. Genet.* **2001**, *43*, 113−124.

(16) Sali, A.; Overington, J. P. Derivation of rules for comparative protein modeling from a database of protein structure alignments. *Protein Sci.* **1994**, *3*, 1582−1596.

(17) Sali, A.; Potterton, L.; Yuan, F.; van Vlijmen, H.; Karplus, M. Evaluation of comparative protein modeling by MODELLER. *Proteins* **1995**, *23*, 318−326.

(18) Insight2000; Accelrys, Inc.: San Diego, CA.

(19) Catalyst4.5; Accelrys Inc.: San Diego, CA.

(20) Gehlhaar, D. K.; Verkhivker, G. M.; Rejto, P. A.; Sherman, C. J.; Fogel, D. B.; Fogel, L. J.; Freer, S. T. Molecular recognition of the inhibitor AG-1343 by HIV-1 protease: conformationally flexible docking by evolutionary programming. *Chem., Biol.* **1995**, *2*, 317−324.

(21) Cerius2; Accelrys, Inc.: San Diego, CA.

(22) Boehm, J. C.; Smietana, J. M.; Sorenson, M. E.; Garigipati, R. S.; Gallagher, T. F.; Sheldrake, P. L.; Bradbeer, J.; Badger, A. M.; Laydon, J. T.; Lee, J. C.; Hillegass, L. M.; Griswold, D. E.; Breton, J. J.; Chabot-Fletcher, M. C.; Adams, J. L. 1-substituted 4-aryl-5-pyridinylimidazoles: a new class of cytokine suppressive drugs with low 5-lipoxygenase and cyclooxygenase inhibitory potency. *J. Med. Chem.* **1996**, *39*, 3929−3937.

(23) Bold, G.; Altmann, K.-H.; Frei, J.; Lang, M.; Manley, P. W.; Traxler, P.; Wietfeld, B.; Brueggen, J.; Buchdunger, E.; Cozens, R.; Ferrari, S.; Furet, P.; Hofmann, F.; Martiny-Baron, G.; Mestan, J.; Roesel, J.; Sills, M.; Stover, D.; Acemoglu, F.; Boss, E.; Emmenegger, R.; Laesser, L.; Masso, E.; Roth, R.; Schlachter, C.; Vetterli, W.; Wyss, D.; Wood, J. M. New Anilinophthalazines as Potent and Orally Well Absorbed Inhibitors of the VEGF Receptor Tyrosine Kinases Useful as Antagonists of Tumor-Driven Angiogenesis. *J. Med. Chem.* **2000**, *43*, 2310−2323.

(24) Boschelli, D. H.; Wu, Z.; Klutchko, S. R.; Showalter, H. D.; Hamby, J. M.; Lu, G. H.; Major, T. C.; Dahring, T. K.; Batley, B.; Panek, R. L.; Keiser, J.; Hartl, B. G.; Kraker, A. J.; Klohs, W. D.; Roberts, B. J.; Patmore, S.; Elliott, W. L.; Steinkampf, R.; Bradford, L. A.; Hallak, H.; Doherty, A. M. Synthesis and tyrosine kinase inhibitory activity of a series of 2-amino-8H-pyrido[2,3-d]pyrimidines: identification of potent, selective platelet-derived growth factor receptor tyrosine kinase inhibitors. *J. Med. Chem.* **1998**, *41*, 4365−4377.

(25) Bridges, A. J.; Zhou, H.; Cody, D. R.; Rewcastle, G. W.; McMichael, A.; Showalter, H. D.; Fry, D. W.; Kraker, A. J.; Denny, W. A. Tyrosine kinase inhibitors. 8. An unusually steep structure−activity relationship for analogues of 4-(3-bromoanilino)-6,7-dimethoxyquinazoline (PD 153035), a potent inhibitor of the epidermal growth factor receptor. *J. Med. Chem.* **1996**, *39*, 267−276.

(26) Connolly, C. J. C.; Hamby, J. M.; Schroeder, M. C.; Barvian, M.; Lu, G. H.; Panek, R. L.; Amar, A.; Shen, C.; Kraker, A. J.; Fry, D. W.; Klohs, W. D.; Doherty, A. M. Discovery and structure−activity studies of a novel series of pyrido[2,3-d]pyrimidine tyrosine kinase inhibitors. *Bioorg. Med. Chem. Lett.* **1997**, *7*, 2415−2420.

(27) de Laszlo, S. E.; Visco, D.; Agarwal, L.; Chang, L.; Chin, J.; Croft, G.; Forsyth, A.; Fletcher, D.; Frantz, B.; Hacker, C.; Hanlon, W.; Harper, C.; Kostura, M.; Li, B.; Luell, S.; MacCoss, M.; Mantlo, N.; O'Neill, E. A.; Orevillo, C.; Pang, M.; Parsons, J.; Rolando, A.; Sahly, Y.; Sidler, K.; O'Keefe, S. J.; et al. Pyrroles and other heterocycles as inhibitors of p38 kinase. *Bioorg. Med. Chem. Lett.* **1998**, *8*, 2689−2694.

(28) Dolle, R. E.; Dunn, J. A.; Bobko, M.; Singh, B.; Kuster, J. E.; Baizman, E.; Harris, A. L.; Sawutz, D. G.; Miller, D.; Wang, S.; et al. 5,7-Dimethoxy-3-(4-pyridinyl)quinoline is a potent and selective inhibitor of human vascular beta-type platelet-derived growth factor receptor tyrosine kinase. *J. Med. Chem.* **1994**, *37*, 2627−2629.

(29) Dumas, J.; Hatoum-Mokdad, H.; Sibley, R.; Riedl, B.; Scott, W. J.; Monahan, M. K.; Lowinger, T. B.; Brennan, C.; Natero, R.; Turner, T.; Johnson, J. S.; Schoenleber, R.; Bhargava, A.; Wilhelm, S. M.; Housley, T. J.; Ranges, G. E.; Shrikhande, A. 1-Phenyl-5-pyrazolyl ureas: potent and selective p38 kinase inhibitors. *Bioorg. Med. Chem. Lett.* **2000**, *10*, 2051−2054.

(30) Dumas, J.; Sibley, R.; Riedl, B.; Monahan, M. K.; Lee, W.; Lowinger, T. B.; Redman, A. M.; Johnson, J. S.; Kingery-Wood, J.; Scott, W. J.; Smith, R. A.; Bobko, M.; Schoenleber, R.; Ranges, G. E.; Housley, T. J.; Bhargava, A.; Wilhelm, S. M.; Shrikhande, A. Discovery of a new class of p38 kinase inhibitors. *Bioorg. Med. Chem. Lett.* **2000**, *10*, 2047−2050.

(31) Gallagher, T. F.; Seibel, G. L.; Kassis, S.; Laydon, J. T.; Blumenthal, M. J.; Lee, J. C.; Lee, D.; Boehm, J. C.; Fier-Thompson, S. M.; Abt, J. W.; Soreson, M. E.; Smietana, J. M.; Hall, R. F.; Garigipati, R. S.; Bender, P. E.; Erhard, K. F.; Krog, A. J.; Hofmann, G. A.; Sheldrake, P. L.; McDonnell, P. C.; Kumar, S.; Young, P. R.; Adams, J. L. Regulation of stress-induced cytokine production by pyridinylimidazoles; inhibition of CSBP kinase. *Bioorg. Med. Chem.* **1997**, *5*, 49−64.

(32) Gibson, K. H.; Brundy, W.; Godfrey, A. A.; Woodburn, J. R.; Ashton, S. E.; Curry, B. J.; Scarlett, L.; Barker, A. J.; Brown, D. S. Epidermal growth factor receptor tyrosine kinase: structure−activity relationships and antitumor activity of novel quinazolines. *Bioorg. Med. Chem. Lett.* **1997**, *7*, 2723−2728.

(33) Hamby, J. M.; Connolly, C. J.; Schroeder, M. C.; Winters, R. T.; Showalter, H. D.; Panek, R. L.; Major, T. C.; Olsewski, B.; Ryan, M. J.; Dahring, T.; Lu, G. H.; Keiser, J.; Amar, A.; Shen, C.; Kraker, A. J.; Slintak, V.; Nelson, J. M.; Fry, D. W.; Bradford, L.; Hallak, H.; Doherty, A. M. Structure−activity relationships for a novel series of pyrido[2,3-d]pyrimidine tyrosine kinase inhibitors. *J. Med. Chem.* **1997**, *40*, 2296−2303.

(34) Hennequin, L. F.; Thomas, A. P.; Johnstone, C.; Stokes, E. S.; Ple, P. A.; Lohmann, J. J.; Ogilvie, D. J.; Dukes, M.; Wedge, S. R.; Curwen, J. O.; Kendrew, J.; Lambert-van der Brempt, C. Design and structure−activity relationship of a new class of potent VEGF receptor tyrosine kinase inhibitors. *J. Med. Chem.* **1999**, *42*, 5369−5389.

(35) Henry, J. R.; Rupert, K. C.; Dodd, J. H.; Turchi, I. J.; Wadsworth, S. A.; Cavender, D. E.; Fahmy, B.; Olini, G. C.; Davis, J. E.; Pellegrino-Gensey, J. L.; Schafer, P. H.; Siekierka, J. J. 6-Amino-2-(4-fluorophenyl)-4-methoxy-3-(4-pyridyl)-1*H*-pyrrolo[2,3-*b*]pyridine (RWJ 68354): a potent and selective p38 kinase inhibitor. *J. Med. Chem.* **1998**, *41*, 4196−4198.

(36) Henry, J. R.; Rupert, K. C.; Dodd, J. H.; Turchi, I. J.; Wadsworth, S. A.; Cavender, D. E.; Schafer, P. H.; Siekierka, J. J. Potent inhibitors of the MAP kinase p38. *Bioorg. Med. Chem. Lett.* **1998**, *8*, 3335−3340.

(37) Klutchko, S. R.; Hamby, J. M.; Boschelli, D. H.; Wu, Z.; Kraker, A. J.; Amar, A. M.; Hartl, B. G.; Shen, C.; Klohs, W. D.; Steinkampf, R. W.; Driscoll, D. L.; Nelson, J. M.; Elliott, W. L.; Roberts, B. J.; Stoner, C. L.; Vincent, P. W.; Dykes, D. J.; Panek, R. L.; Lu, G. H.; Major, T. C.; Dahring, T. K.; Hallak, H.; Bradford, L. A.; Showalter, H. D. H.; Doherty, A. M. 2-Substituted Aminopyrido[2,3-*d*]pyrimidin-7(8*H*)-ones. Structure−Activity Relationships Against Selected Tyrosine Kinases and in Vitro and in Vivo Anticancer Activity. *J. Med. Chem.* **1998**, *41*, 3276−3292.

(38) Liverton, N. J.; Butcher, J. W.; Claiborne, C. F.; Claremon, D. A.; Libby, B. E.; Nguyen, K. T.; Pitzenberger, S. M.; Selnick, H. G.; Smith, G. R.; Tebben, A.; Vacca, J. P.; Varga, S. L.; Agarwal, L.; Dancheck, K.; Forsyth, A. J.; Fletcher, D. S.; Frantz, B.;

Hanlon, W. A.; Harper, C. F.; Hofsess, S. J.; Kostura, M.; Lin, J.; Luell, S. O.; Neill, E. A. O.; Keefe, S. J. Design and synthesis of potent, selective, and orally bioavailable tetrasubstituted imidazole inhibitors of p38 mitogen-activated protein kinase. *J. Med. Chem.* **1999**, *42*, 2180−2190.

(39) Maguire, M. P.; Sheets, K. R.; McVety, K.; Spada, A. P.; Zilberstein, A. A new series of PDGF receptor tyrosine kinase inhibitors: 3-substituted quinoline derivatives. *J. Med. Chem.* **1994**, *37*, 2129−2137.

(40) Missbach, M.; Altmann, E.; Widler, L.; Susa, M.; Buchdunger, E.; Mett, H.; Meyer, T.; Green, J. Substituted 5,7-diphenylpyrrolo[2,3-d]pyrimidines: potent inhibitors of the tyrosine kinase c-Src. *Bioorg. Med. Chem. Lett.* **2000**, *10*, 945−949.

(41) Myers, M. R.; Setzer, N. N.; Spada, A. P.; Persons, P. E.; Ly, C. Q.; Maguire, M. P.; Zulli, A. L.; Cheney, D. L.; Zilberstein, A.; Johnson, S. E.; Franks, C. F.; Mitchell, K. J. The synthesis and SAR of new 4-(N-alkyl-N-phenyl)amino-6,7-dimethoxyquinazolines and 4-(N-alkyl-N-phenyl)aminopyrazolo[3,4-d]pyrimidines, inhibitors of CSF-1R tyrosine kinase activity. *Bioorg. Med. Chem. Lett.* **1997**, *7*, 421−424.

(42) Myers, M. R.; Setzer, N. N.; Spada, A. P.; Zulli, A. L.; Hsu, C.-Y. J.; Zilberstein, A.; Johnson, S. E.; Hook, L. E.; Jacoski, M. V. The preparation and SAR of 4-(anilino), 4-(phenoxy), and 4-(thiophenoxy)-quinazolines: inhibitors of p56lck and EGF−R tyrosine kinase activity. *Bioorg. Med. Chem. Lett.* **1997**, *7*, 417−420.

(43) Palmer, B. D.; Trumpp-Kallmeyer, S.; Fry, D. W.; Nelson, J. M.; Showalter, H. D.; Denny, W. A. Tyrosine kinase inhibitors. 11. Soluble analogues of pyrrolo- and pyrazoloquinazolines as epidermal growth factor receptor inhibitors: synthesis, biological evaluation, and modeling of the mode of binding. *J. Med. Chem.* **1997**, *40*, 1519−1529.

(44) Palmer, B. D.; Smaill, J. B.; Boyd, M.; Boschelli, D. H.; Doherty, A. M.; Hamby, J. M.; Khatana, S. S.; Kramer, J. B.; Kraker, A. J.; Panek, R. L.; Lu, G. H.; Dahring, T. K.; Winters, R. T.; Showalter, H. D. H.; Denny, W. A. Structure−activity relationships for 1-phenylbenzimidazoles as selective ATP site inhibitors of the platelet-derived growth factor receptor. *J. Med. Chem.* **1998**, *41*, 5457−5465.

(45) Palmer, B. D.; Kraker, A. J.; Hartl, B. G.; Panopoulos, A. D.; Panek, R. L.; Batley, B. L.; Lu, G. H.; Trumpp-Kallmeyer, S.; Showalter, H. D. H.; Denny, W. A. Structure−Activity Relationships for 5-Substituted 1-Phenylbenzimidazoles as Selective Inhibitors of the Platelet-Derived Growth Factor Receptor. *J. Med. Chem.* **1999**, *42*, 2373−2382.

(46) Revesz, L.; Di Padova, F. E.; Buhl, T.; Feifel, R.; Gram, H.; Hiestand, P.; Manning, U.; Zimmerlin, A. G. SAR of 4-hydroxypiperidine and hydroxyalkyl substituted heterocycles as novel p38 Map kinase inhibitors. *Bioorg. Med. Chem. Lett.* **2000**, *10*, 1261−1264.

(47) Rewcastle, G. W.; Denny, W. A.; Bridges, A. J.; Zhou, H.; Cody, D. R.; McMichael, A.; Fry, D. W. Tyrosine kinase inhibitors. 5. Synthesis and structure−activity relationships for 4-[(phenylmethyl)amino]- and 4-(phenylamino)quinazolines as potent adenosine 5′-triphosphate binding site inhibitors of the tyrosine kinase domain of the epidermal growth factor receptor. *J. Med. Chem.* **1995**, *38*, 3482−3487.

(48) Rewcastle, G. W.; Palmer, B. D.; Bridges, A. J.; Showalter, H. D.; Sun, L.; Nelson, J.; McMichael, A.; Kraker, A. J.; Fry, D. W.; Denny, W. A. Tyrosine kinase inhibitors. 9. Synthesis and evaluation of fused tricyclic quinazoline analogues as ATP site inhibitors of the tyrosine kinase activity of the epidermal growth factor receptor. *J. Med. Chem.* **1996**, *39*, 918−928.

(49) Rewcastle, G. W.; Palmer, B. D.; Thompson, A. M.; Bridges, A. J.; Cody, D. R.; Zhou, H.; Fry, D. W.; McMichael, A.; Denny, W. A. Tyrosine kinase inhibitors. 10. Isomeric 4-[(3-bromophenyl)amino]pyrido[d]-pyrimidines are potent ATP binding site inhibitors of the tyrosine kinase function of the epidermal growth factor receptor. *J. Med. Chem.* **1996**, *39*, 1823−1835.

(50) Rewcastle, G. W.; Bridges, A. J.; Fry, D. W.; Rubin, J. R.; Denny, W. A. Tyrosine kinase inhibitors. 12. Synthesis and structure−activity relationships for 6-substituted 4-(phenylamino)pyrimido-[5,4-d]pyrimidines designed as inhibitors of the epidermal growth factor receptor. *J. Med. Chem.* **1997**, *40*, 1820−1826.

(51) Rewcastle, G. W.; Murray, D. K.; Elliott, W. L.; Fry, D. W.; Howard, C. T.; Nelson, J. M.; Roberts, B. J.; Vincent, P. W.; Showalter, H. D.; Winters, R. T.; Denny, W. A. Tyrosine kinase inhibitors. 14. Structure−activity relationships for methylamino-substituted derivatives of 4-[(3-bromophenyl)amino]-6-(methylamino)-pyrido[3,4-*d*]pyrimidine (PD 158780), a potent and specific inhibitor of the tyrosine kinase activity of receptors for the EGF family of growth factors. *J. Med. Chem.* **1998**, *41*, 742−751.

(52) Showalter, H. D.; Bridges, A. J.; Zhou, H.; Sercel, A. D.; McMichael, A.; Fry, D. W. Tyrosine kinase inhibitors. 16. 6,5,6-tricyclic benzothieno[3,2-*d*]pyrimidines and pyrimido[5,4-*b*]- and -[4,5-*b*]indoles as potent inhibitors of the epidermal growth factor receptor tyrosine kinase. *J. Med. Chem.* **1999**, *42*, 5464−5474.

(53) Sun, L.; Tran, N.; Liang, C.; Tang, F.; Rice, A.; Schreck, R.; Waltz, K.; Shawver, L. K.; McMahon, G.; Tang, C. Design, synthesis, and evaluations of substituted 3-[(3- or 4-carboxyethylpyrrol-2-yl)methylidenyl]indolin-2-ones as inhibitors of VEGF, FGF, and PDGF receptor tyrosine kinases. *J. Med. Chem.* **1999**, *42*, 5120−5130.

(54) Sun, L.; Tran, N.; Liang, C.; Hubbard, S.; Tang, F.; Lipson, K.; Schreck, R.; Zhou, Y.; McMahon, G.; Tang, C. Identification of substituted 3-[(4,5,6,7-tetrahydro-1*H*-indol-2-yl)methylene]-1,3-dihydroindol-2-ones as growth factor receptor inhibitors for VEGF−R2 (Flk-1/KDR), FGF−R1, and PDGF-Rbeta tyrosine kinases. *J. Med. Chem.* **2000**, *43*, 2655−2663.

(55) Thompson, A. M.; Bridges, A. J.; Fry, D. W.; Kraker, A. J.; Denny, W. A. Tyrosine kinase inhibitors. 7. 7-Amino-4-(phenylamino)- and 7-amino-4-[(phenylmethyl)amino]pyrido[4,3-d]pyrimidines: a new class of inhibitors of the tyrosine kinase activity of the epidermal growth factor receptor. *J. Med. Chem.* **1995**, *38*, 3780−3788.

(56) Thompson, A. M.; Murray, D. K.; Elliott, W. L.; Fry, D. W.; Nelson, J. A.; Showalter, H. D.; Roberts, B. J.; Vincent, P. W.; Denny, W. A. Tyrosine kinase inhibitors. 13. Structure−activity relationships for soluble 7-substituted 4-[(3-bromophenyl)amino]-pyrido[4,3-d]pyrimidines designed as inhibitors of the tyrosine kinase activity of the epidermal growth factor receptor. *J. Med. Chem.* **1997**, *40*, 3915−3925.

(57) Thompson, A. M.; Rewcastle, G. W.; Boushelle, S. L.; Hartl, B. G.; Kraker, A. J.; Lu, G. H.; Batley, B. L.; Panek, R. L.; Showalter, H. D. H.; Denny, W. A. Synthesis and Structure−Activity Relationships of 7-Substituted 3-(2,6-Dichlorophenyl)-1,6-naphthyridin-2(1H)-ones as Selective Inhibitors of pp60c-src. *J. Med. Chem.* **2000**, *43*, 3134−3147.

(58) Thompson, A. M.; Connolly, C. J.; Hamby, J. M.; Boushelle, S.; Hartl, B. G.; Amar, A. M.; Kraker, A. J.; Driscoll, D. L.; Steinkampf, R. W.; Patmore, S. J.; Vincent, P. W.; Roberts, B. J.; Elliott, W. L.; Klohs, W.; Leopold, W. R.; Showalter, H. D.; Denny, W. A. 3-(3,5-Dimethoxyphenyl)-1,6-naphthyridine-2,7-diamines and Related 2-Urea Derivatives Are Potent and Selective Inhibitors of the FGF Receptor-1 Tyrosine Kinase. *J. Med. Chem.* **2000**, *43*, 4200−4211.

(59) Traxler, P. M.; Furet, P.; Mett, H.; Buchdunger, E.; Meyer, T.; N., L. 4-(Phenylamino)pyrrolopyrimidines: potent and selective, ATP site directed inhibitors of the EGF-receptor protein tyrosine kinase. *J. Med. Chem.* **1996**, *39*, 2285−2292.

(60) Traxler, P.; Green, J.; Mett, H.; Sequin, U.; P., F. Use of a pharmacophore model for the design of EGFR tyrosine kinase inhibitors: isoflavones and 3-phenyl-4(1*H*)-quinolones. *J. Med. Chem.* **1999**, *42*, 1018−1026.

(61) Wissner, A.; Berger, D. M.; Boschelli, D. H.; Floyd, M. B., Jr.; Greenberger, L. M.; Gruber, B. C.; Johnson, B. D.; Mamuya, N.; Nilakantan, R.; Reich, M. F.; Shen, R.; Tsou, H. R.; Upeslacis, E.; Wang, Y. F.; Wu, B.; Ye, F.; Zhang, N. 4-Anilino-6,7-dialkoxyquinoline-3-carbonitrile inhibitors of epidermal growth factor receptor kinase and their bioisosteric relationship to the 4-anilino-6,7-dialkoxyquinazoline inhibitors. *J. Med. Chem.* **2000**, *43*, 3244−3256.

(62) Zimmermann, J.; Buchdunger, E.; Mett, H.; Meyer, T.; Lydon, N. B.; Traxler, P. (Phenylamino)pyrimidine (PAP) derivatives: a new class of potent and highly selective PDGF-receptor autophosphorylation inhibitors. *Bioorg. Med. Chem. Lett.* **1996**, *6*, 1221−1226.

(63) Zimmermann, J.; Buchdunger, E.; Mett, H.; Meyer, T.; Lydon, N. B. Potent and selective inhibitors of the ABL-kinase: phenylaminopyrimidine (PAP) derivatives. *Bioorg. Med. Chem. Lett.* **1997**, *7*, 187−192.

(64) Wang, J.; Szewczuk, Z.; Yue, S. Y.; Tsuda, Y.; Konishi, Y.; Purisima, E. O. Calculation of relative binding free energies and configurational entropies: a structural and thermodynamic analysis of the nature of nonpolar binding of thrombin inhibitors based on hirudin55−65. *J. Mol. Biol.* **1995**, *253*, 473−492.

(65) Penel, S.; Doig, A. J. Rotamer strain energy in protein helices − quantification of a major force opposing protein folding. *J. Mol. Biol.* **2001**, *305*, 961−968.

(66) Bohm, H. J. The development of a simple empirical scoring function to estimate the binding constant for a protein−ligand complex of known three-dimensional structure. *J. Comput. Aided Mol. Des.* **1994**, *8*, 243−256.

(67) D'Aquino, J. A.; Freire, E.; Amzel, L. M. Binding of small organic molecules to macromolecular targets: evaluation of conformational entropy changes. *Proteins* **2000**, *Suppl*, 93−107.

(68) Stouten, P. F. W.; Froemmel, C.; Nakamura, H.; Sander, C. An effective solvation term based on atomic occupancies for use in protein simulations. *Mol. Simul.* **1993**, *10*, 97−120.

(69) Guner, O. F. *Pharmacophore Perception, Development and Use in Drug Design.*; International University Line: La Jolla, CA, 1999; p 537.

(70) Stamos, J.; Sliwkowski, M. X.; Eigenbrot, C. Structure of the epidermal growth factor receptor kinase domain alone and in complex with a 4-anilinoquinazoline inhibitor. *J. Biol. Chem.* **2002**, *277*, 46265−46272.
(71) Wang, Z.; Canagarajah, B. J.; Boehm, J. C.; Kassisa, S.; Cobb, M. H.; Young, P. R.; Abdel-Meguid, S.; Adams, J. L.; Goldsmith, E. J. Structural basis of inhibitor selectivity in MAP kinases. *Structure* **1998**, *6*, 1117−1128.
(72) Yamaguchi, H.; Hendrickson, W. A. Structural basis for activation of human lymphocyte kinase Lck upon tyrosine phosphorylation. *Nature* **1996**, *384*, 484−489.
(73) Schindler, T.; Bornmann, W.; Pellicena, P.; Miller, W. T.; Clarkson, B.; Kuriyan, J. Structural mechanism for STI-571 inhibition of abelson tyrosine kinase. *Science* **2000**, *289*, 1938−1942.
(74) Pargellis, C.; Tong, L.; Churchill, L.; Cirillo, P. F.; Gilmore, T.; Graham, A. G.; Grob, P. M.; Hickey, E. R.; Moss, N.; Pav, S.; Regan, J. Inhibition of p38 MAP kinase by utilizing a novel allosteric binding site. *Nat. Struct. Biol.* **2002**, *9*, 268−272.
(75) Mohammadi, M.; Froum, S.; Hamby, J. M.; Schroeder, M. C.; Panek, R. L.; Lu, G. H.; Eliseenkova, A. V.; Green, D.; Schlessinger, J.; Hubbard, S. R. Crystal structure of an angiogenesis inhibitor bound to the FGF receptor tyrosine kinase domain. *EMBO J.* **1998**, *17*, 5896−5904.
(76) Hubbard, S. R. Crystal structure of the activated insulin receptor tyrosine kinase in complex with peptide substrate and ATP analog. *EMBO J.* **1997**, *16*, 5572−5581.

JM020503A